


## Article

# Activation of a Sweet Taste Receptor by Oleanane-Type Glycosides from *Wisteria sinensis*

Samir Hobloss<sup>1</sup>, Antoine Bruguière<sup>1</sup>, David Pertuit<sup>1</sup>, Tomofumi Miyamoto<sup>2</sup>, Chiaki Tanaka<sup>2</sup>, Christine Belloir<sup>1</sup> , Marie-Aleth Lacaille-Dubois<sup>1</sup>, Loïc Briand<sup>1</sup> and Anne-Claire Mitaine-Offer<sup>1,\*</sup>

<sup>1</sup> Centre des Sciences du Goût et de l'Alimentation, CNRS, INRAE, Institut Agro, Université de Bourgogne, Franche-Comté, 21000 Dijon, France

<sup>2</sup> Graduate School of Pharmaceutical Sciences, Kyushu University, Fukuoka 812-8582, Japan

\* Correspondence: anne-claire.offer@u-bourgogne.fr

**Abstract:** The phytochemical study of *Wisteria sinensis* (Sims) DC. (Fabaceae), commonly known as the Chinese Wisteria, led to the isolation of seven oleanane-type glycosides from an aqueous-ethanolic extract of the roots. Among the seven isolated saponins, two have never been reported before: 3-O- $\alpha$ -L-rhamnopyranosyl-(1 $\rightarrow$ 2)- $\beta$ -D-glucopyranosyl-(1 $\rightarrow$ 2)- $\beta$ -D-glucuronopyranosyl-22-O-acetylolean-12-ene-3 $\beta$ ,16 $\beta$ ,22 $\beta$ ,30-tetrol, and 3-O- $\beta$ -D-xylopyranosyl-(1 $\rightarrow$ 2)- $\beta$ -D-glucuronopyranosyl-wistariasapogenol A. Based on the close structures between the saponins from *W. sinensis*, and the glycyrrhizin from licorice, the stimulation of the sweet taste receptor TAS1R2/TAS1R3 by these glycosides was evaluated.

**Keywords:** *Wisteria sinensis*; Fabaceae; triterpene glycosides; sweet taste; TAS1R2/TAS1R3



**Citation:** Hobloss, S.; Bruguière, A.; Pertuit, D.; Miyamoto, T.; Tanaka, C.; Belloir, C.; Lacaille-Dubois, M.-A.; Briand, L.; Mitaine-Offer, A.-C. Activation of a Sweet Taste Receptor by Oleanane-Type Glycosides from *Wisteria sinensis*. *Molecules* **2022**, *27*, 7866. <https://doi.org/10.3390/molecules27227866>

Academic Editors: Vladimir A. Khrpach and Pavel B. Drašar

Received: 19 October 2022

Accepted: 9 November 2022

Published: 15 November 2022

**Publisher's Note:** MDPI stays neutral with regard to jurisdictional claims in published maps and institutional affiliations.



**Copyright:** © 2022 by the authors. Licensee MDPI, Basel, Switzerland. This article is an open access article distributed under the terms and conditions of the Creative Commons Attribution (CC BY) license (<https://creativecommons.org/licenses/by/4.0/>).

## 1. Introduction

Since the end of the 20th century, obesity has been one of the biggest health problems worldwide and has been linked in the long term to many different diseases such as type 2 diabetes, cardiovascular disease, hypertension, metabolic syndrome, and dyslipidemia [1,2]. However, reducing sugar intake can be very difficult, knowing that people's taste preference for sweetness is innate [3]. Thus, to limit the prevalence of diseases linked to this excessive consumption of sugar, the search for natural non-caloric compounds with a sweet taste and the development of artificial sweeteners has increased [4]. Some natural triterpene glycosides activate sweet taste receptors, such as glycyrrhizin from licorice (*Glycyrrhiza glabra* L., Fabaceae), which stimulates the heterodimer TAS1R2/TAS1R3 [5,6]. The Fabaceae family is one of the most important families of Angiosperms, being the third largest of this group with 727 genera and about 19,325 species [7]. From a chemotaxonomic point of view, the two genera *Wisteria* Nutt. and *Glycyrrhiza* L. belong to the Faboideae subfamily, so they are phylogenetically very close [8]. Moreover, oleanane-type glycosides isolated from *Wisteria* species like *W. frutescens* [9], *W. floribunda* cultivars [10], and *W. brachybotrys* [11], showed some structural similarities with glycyrrhizin [12]: a  $\beta$ -carboxyl group at position C-30, a ketone function, and a 3-O- $\beta$ -D-glucuronopyranosyl moiety.

Therefore, the aim of this paper is the isolation and the structural analysis of oleanane glycosides from the Chinese Wisteria, *W. sinensis* (Sims) DC., as well as the evaluation of their sweet taste by cell-based receptors assays. Seven saponins were purified after an extraction of the roots, and their structures were established. Two previously undescribed (1,2) and five known ones (3–7) (Figure 1) were reported, as 3-O- $\alpha$ -L-rhamnopyranosyl-(1 $\rightarrow$ 2)- $\beta$ -D-glucopyranosyl-(1 $\rightarrow$ 2)- $\beta$ -D-glucuronopyranosyl-22-O-acetylolean-12-ene-3 $\beta$ ,16 $\beta$ ,22 $\beta$ ,30-tetrol (1), 3-O- $\beta$ -D-xylopyranosyl-(1 $\rightarrow$ 2)- $\beta$ -D-glucuronopyranosyl-wistariasapogenol A (2), wistariasapogenin A (3) [13], wistariasapogenin D (4) [11], dehydroazukisapogenin V (5) [14], astragaloside VIII (6) [15], and azukisapogenin V (7) [14]. Compounds 1–3 have been tested on the TAS1R2/TAS1R3 receptor to establish structure–activity relationships.

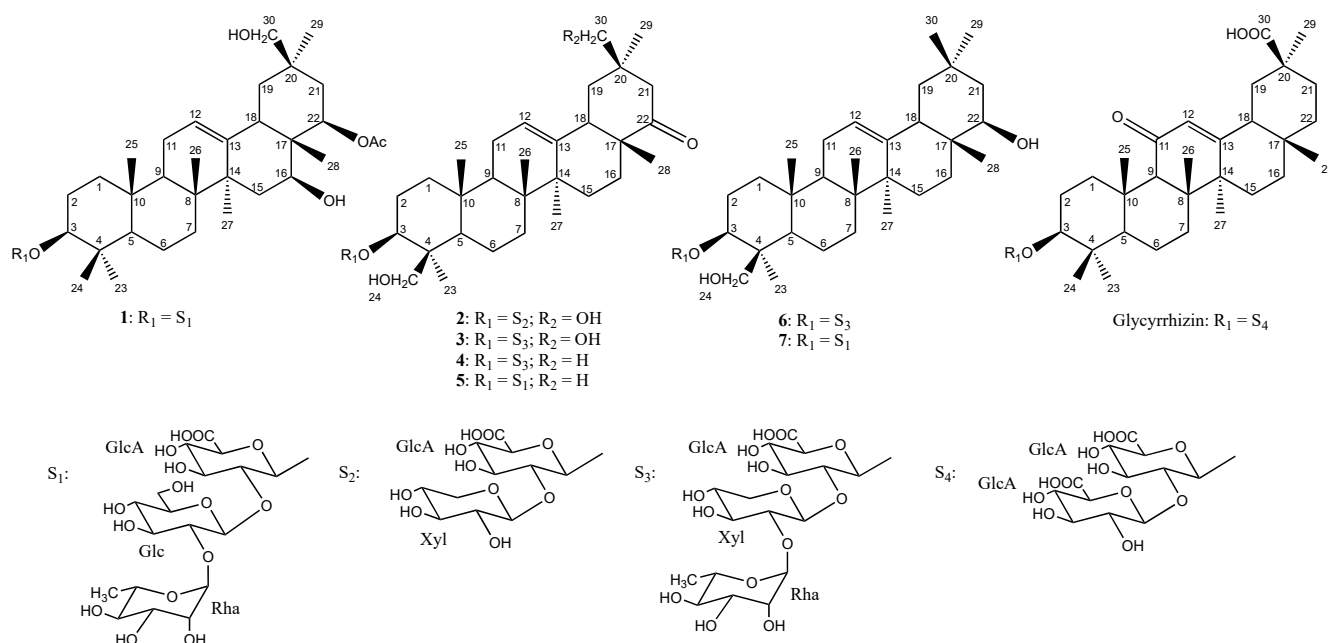


**Figure 1.** Structures of compounds 1–7 and glycyrrhizin.

## 2. Results and Discussion

The saponins 1–7 were isolated from an aqueous-ethanolic extract of the roots of *W. sinensis* by various solid/liquid chromatographic methods, vacuum liquid chromatography (VLC), medium pressure liquid chromatography (MPLC), on normal and reverse phase RP-18 silica gel, and size exclusion chromatography on Sephadex LH-20.

The mass spectrum of compound 1 in HRESIMS (positive mode), reveals a quasi-molecular ion at  $m/z$  1023.5051 [ $M + Na$ ]<sup>+</sup>, in agreement with the molecular formula  $C_{50}H_{80}O_{20}Na$ . This suggests a molecular mass of 1000 g/mol.

The structure of the aglycone was determined using 1D and 2D NMR spectra, mainly COSY, TOCSY, ROESY, HSQC and HMBC (Table 1).

**Table 1.** <sup>13</sup>C NMR and <sup>1</sup>H NMR data of compounds 1–2 in MeOD ( $\delta$  ppm,  $J$  in Hz) <sup>1</sup>.

Position	1		2	
	$\delta_C$	$\delta_H$ ( $J$ in Hz)	$\delta_C$	$\delta_H$ ( $J$ in Hz)
1	38.5	1.02 m 1.64 m	38.4	1.02 m 1.63 m
2	25.4	1.72 m 2.13 m	25.5	2.10 m 2.13 m
3	90.4	3.22	90.3	3.35 dd (11.7, 2.9)
4	39.1	-	43.3	-
5	55.5	0.80	56.0	0.95
6	17.9	1.44 m 1.59 m	18.0	1.41 m 1.66 m
7	32.4	1.37 m 1.59 m	32.6	1.40 m 1.58 m
8	39.8	-	39.4	-
9	46.8	1.57 m	47.8	1.62 m
10	36.3	-	36.1	-
11	23.2	1.91 m 1.93 m	23.4	1.90 m 1.92 m
12	123.0	5.33 br t (3.0)	123.8	5.38 br t (3.0)
13	142.3	-	141.4	-
14	42.9	-	41.6	-

Table 1. Cont.

Position	1		2	
	$\delta_C$	$\delta_H$ (J in Hz)	$\delta_C$	$\delta_H$ (J in Hz)
15	35.9	1.31 m 1.76 m	24.8	1.11 m 1.79 m
16	66.2	4.15 dd (11.7, 4.7)	26.7	1.21 m 2.07 m
17	41.0	-	46.9	-
18	45.7	2.33 dd (14.1, 4.1)	46.9	2.46 dd (13.5, 3.5)
19	40.5	1.34 1.73	41.8	1.62 1.99
20	34.5	-	38.6	-
21	32.8	1.49 1.75	46.0	2.18 d (14.4) 2.36 d (14.4)
22	74.2	5.24 dd (3.5, 1.2)	218.0	-
23	15.4	0.88 s	21.3	1.18 s
24	27.3	1.11 s	62.5	3.23 d (12.0) 4.06 d (12.0)
25	14.7	0.98 s	14.7	0.88 s
26	16.1	1.02 s	16.0	0.97 s
27	26.5	1.26 s	24.3	1.24 s
28	13.8	0.79 s	19.9	0.97 s
29	27.0	0.91 s	25.4	0.93 s
30	67.3	3.49 d (14.1) 3.51 d (14.1)	67.4	3.28 d (12.9) 3.34 d (12.9)
at C-22				
COCH <sub>3</sub>	171.1	-		
CH <sub>3</sub> CO	20.0	2.02 (3H, s)		
GlcA-1	104.3	4.42 d (7.6)	103.5	4.45 d (7.6)
2	79.6	3.70 dd (9.4, 7.6)	79.6	3.49 dd (9.4, 7.6)
3	77.3	3.60 t (9.4)	76.7	3.61 t (9.4)
4	72.6	3.42 t (9.4)	72.1	3.48
5	75.1	3.52	75.3	3.60
6	175.3	-	175.7	-
Xyl-1			103.7	4.63 d (7.6)
2			74.1	3.19 dd (9.4, 7.6)
3			77.0	3.28 t (9.4)
4			69.4	3.49 m
5			65.5	3.12 dd (11.1, 9.4) 3.81 dd (11.1, 5.3)
Glc-1	100.7	4.88 d (7.6)		
2	78.2	3.37 dd (9.4, 7.6)		
3	77.9	3.44 t (9.4)		
4	71.3	3.05 t (9.4)		
5	76.7	3.22 m		
6	62.2	3.82 dd (11.7, 2.4) 3.52 dd (11.7, 7.6)		
Rha-1	100.6	5.19 br s		
2	70.9	3.91 br s		
3	70.8	3.75 dd (9.4, 2.9)		
4	72.8	3.39 t (9.4)		
5	68.2	4.12 dq (9.4, 5.9)		
6	16.9	1.25 d (5.9)		

<sup>1</sup> Overlapped signal are reported without designated multiplicity.  $\delta$  in ppm; J in parentheses in Hz.

The <sup>1</sup>H NMR spectrum part of the aglycon displayed signals attributable to seven angular methyl groups (3H, s, each) at  $\delta_H$  0.79 (H-28), 0.88 (H-23), 0.91 (H-29), 0.98 (H-25), 1.02 (H-26), 1.11 (H-24) and 1.26 (H-27), one olefinic proton at  $\delta_H$  5.33 (1H, br t, J = 3.0 Hz, H-12), three secondary alcoholic functions at  $\delta_H$  3.22 (1H, H-3), 4.15 (1H, dd, J = 11.7,

4.7 Hz, H-16) and 5.24 (1H, dd,  $J = 3.5, 1.2$  Hz, H-22) and a primary one at  $\delta_H$  3.49 (1H, d,  $J = 14.1$  Hz, H-30<sub>a</sub>), 3.51 (1H, d,  $J = 14.1$  Hz, H-30<sub>b</sub>). Additionally, an HMBC correlation at  $\delta_H$  2.02 (3H, s)/ $\delta_C$  171.1 revealed the presence of an acetyl group. A classical 3-*O*-glycosidic linkage can be observed according to the deshielded signals of position 3 at  $\delta_H$  3.22 (1H, H-3)/ $\delta_C$  90.4 (C-3). Moreover, a HMBC cross-peak at  $\delta_H$  4.15 (1H, H-16<sub>ax</sub>)/ $\delta_C$  13.8 (C-28), and a COSY correlation between 4.15 (1H, H-16<sub>ax</sub>) and  $\delta_H$  1.31 (1H, H-15<sub>eq</sub>), 1.76 (1H, H-15<sub>ax</sub>), allowed the localization of a secondary alcoholic function at the C-16 position. A deshielded signal of a proton at  $\delta_H$  5.24 suggests an acylation by an acetyl group at  $\delta_H$  2.02 (3H, s)/ $\delta_C$  171.1. The localization of this *O*-acetyl group at the 22-position was determined by an HMBC cross-peak between  $\delta_H$  0.79 (3H, H-28) and  $\delta_C$  74.2 (C-22), and a COSY correlation between  $\delta_H$  5.24 (1H, H-22<sub>eq</sub>) and 1.49 (1H, H-21<sub>a</sub>), 1.75 (1H, H-21<sub>b</sub>). The CH<sub>2</sub>OH group was assigned at the C-30 position according to the HMBC cross-peak at  $\delta_H$  0.91 (3H, H-29)/ $\delta_C$  67.3 (C-30), and the ROESY correlation at  $\delta_H$  2.33 (1H, dd,  $J = 14.1, 4.1$  Hz, H-18)/ $\delta_H$  3.49 (1H, H-30<sub>a</sub>), 3.51 (1H, H-30<sub>b</sub>).

The configurations of C-3 and C-16 were determined by the correlations observed in the ROESY spectrum between the H-3  $\alpha$ -axial and the H-5  $\alpha$ -axial, and between the H-16  $\alpha$ -axial and the H<sub>3</sub>-27  $\alpha$ -axial, respectively (Figure 2). The  $\alpha$ -equatorial orientation of H-22 was established by its low coupling constant value (dd,  $J = 3.5, 1.2$  Hz) and by its ROESY connectivity with H-16  $\alpha$ -axial. The aglycone structure of saponin **1** was therefore recognized as 22-*O*-acetylolean-12-ene-3 $\beta$ ,16 $\beta$ ,22 $\beta$ ,30-tetrol. (Figures S1–S3. <sup>1</sup>H spectrum of compound **1**; Figures S4–S7. <sup>13</sup>C spectrum of compound **1**; Figures S8–S11. HSQC spectrum of compound **1**; Figures S12 and S13. HMBC spectra of compound **1**; Figure S14–S16. COSY spectrum of compound **1**; Figures S17–S19. ROESY spectrum of compound **1**).

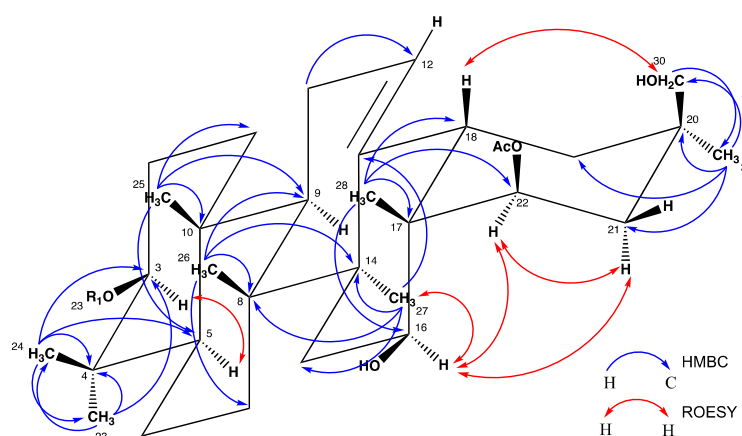


**Figure 2.** Key HMBC and ROESY correlations for the aglycone of **1**.

In the osidic part of compound **1**, the HSQC spectrum showed three anomeric signals at  $\delta_H$  4.42 (1H, d,  $J = 7.6$  Hz)/ $\delta_C$  104.3,  $\delta_H$  4.88 (1H, d,  $J = 7.6$  Hz)/ $\delta_C$  100.7 and  $\delta_H$  5.19 (1H, br s)/ $\delta_C$  100.6. The ring protons of the monosaccharide residues were assigned mainly by COSY, TOCSY, HSQC, and HMBC experiments, which allowed the identification of one glucuronopyranosyl (GlcA), one glucopyranosyl (Glc), and one rhamnopyranosyl (Rha) units (Table 1). The large  $^3J_{H-1,H-2}$  values in the <sup>1</sup>H NMR spectrum of glucuronic acid and glucose in their pyranose form (7.6 Hz) indicated their  $\beta$  anomeric orientation. The large  $^1J_{H-1,C-1}$  value of the Rha (167 Hz) confirmed that the anomeric proton was equatorial ( $\alpha$ -pyranoid anomeric form). The absolute configurations of the sugars were determined to be D for GlcA and Glc, and L for Rha (Experimental section). The same protocol was used for the identification of the monosaccharides of compound **2**.

The HMBC correlations at  $\delta_H$  3.70 (1H, dd,  $J = 9.4, 7.6$  Hz, GlcA-2)/ $\delta_C$  100.7 (Glc-1) and at  $\delta_H$  3.37 (1H, dd,  $J = 9.4, 7.0$  Hz, Glc-2)/ $\delta_C$  100.6 (Rha 1) suggest an  $\alpha$ -L-rhamnopyranosyl-(1 $\rightarrow$ 2)- $\beta$ -D-glucopyranosyl-(1 $\rightarrow$ 2)- $\beta$ -D-glucuronopyranosyl sequence (Table 1, Figure 1).

The HMBC correlation at  $\delta_H$  4.42 (1H, GlcA-1)/ $\delta_C$  90.4 (C-3) and the ROESY cross-peak at  $\delta_H$  4.42 (1H, GlcA-1)/ $\delta_H$  3.22 (1H, H-3<sub>ax</sub>), proved a 3-O-heterosidic bond between GlcA and C-3 of the aglycone. Based on the above results, the structure of compound **1** was elucidated as 3-O- $\alpha$ -L-rhamnopyranosyl-(1 $\rightarrow$ 2)- $\beta$ -D-glucopyranosyl-(1 $\rightarrow$ 2)- $\beta$ -D-glucuronopyranosyl-22-O-acetylolean-12-ene-3 $\beta$ ,16 $\beta$ ,22 $\beta$ ,30-tetrol. (Figures S20–S22.  $^1H$  spectrum of compound **2**; Figures S23–S26.  $^{13}C$  spectrum of compound **2**; Figures S27–S30. HSQC spectrum of compound **2**; Figures S31–S34. HMBC spectrum of compound **2**; Figures S35 and S36. COSY spectrum of compound **2**; Figures S37 and S38. ROESY spectrum of compound **2**).

Analysis of the mass spectrum of compound **2** in HRESIMS (positive mode) reveals a quasi-molecular ion at  $m/z$  803.4195  $[M + Na]^+$ , in agreement with the molecular formula of  $C_{41}H_{64}O_{14}Na$ . This suggests a molecular mass of 780 g/mol.

The  $^1H$  NMR spectrum part of the aglycon displayed signals attributable to six angular methyl groups (3H, s, each) at  $\delta_H$  0.88 (H-25), 0.93 (H-29), 0.97 (H-28), 0.97 (H-26), 1.18 (H-23), and 1.24 (H-27), one olefinic proton at  $\delta_H$  5.38 (1H, br t,  $J = 3.0$  Hz, H-12), one secondary alcoholic function at  $\delta_H$  3.35 (1H, dd,  $J = 11.7, 2.9$  Hz, H-3), and two primary ones at  $\delta_H$  3.23 (1H, d,  $J = 12.0$  Hz, H-24<sub>a</sub>), 4.06 (1H, d,  $J = 12.0$  Hz, H-24<sub>b</sub>) and  $\delta_H$  3.28 (1H, d,  $J = 12.9$  Hz, H-30<sub>a</sub>), 3.34 (1H, d,  $J = 12.9$  Hz, H-30<sub>b</sub>) (Table 1). Additionally, HMBC correlations at  $\delta_H$  2.18 (1H, d,  $J = 14.4$  Hz, H-21<sub>a</sub>)/ $\delta_C$  218.0 (C-22) and  $\delta_H$  2.36 (1H, d,  $J = 14.4$  Hz, H-21<sub>b</sub>)/ $\delta_C$  218.0 (C-22), revealed the presence of a ketone function at the 22-position. A deshielded signal corresponding to a 3-O-glycosidic linkage can be observed at position 3 of the aglycon at  $\delta_H$  3.35 (1H, H-3)/ $\delta_C$  90.3 (C-3). Moreover, the first CH<sub>2</sub>OH group was assigned at the C-30 position as in compound **1**, according to the HMBC cross-peak at  $\delta_H$  0.93 (3H, H-29)/ $\delta_C$  67.4 (C-30), and the ROESY correlations at  $\delta_H$  2.46 (1H, dd,  $J = 13.5, 3.5$  Hz, H-18)/ $\delta_H$  3.28 (1H, H-30<sub>a</sub>), 3.34 (1H, H-30<sub>b</sub>). The second CH<sub>2</sub>OH group was located at the C-24 position by the correlation in the HMBC spectrum at  $\delta_H$  1.18 (3H, H-23)/ $\delta_C$  62.5 (C-24), and the ROESY correlations at  $\delta_H$  4.06 (1H, H-24<sub>b</sub>)/ $\delta_H$  0.88 (3H, H-25) and  $\delta_H$  0.97 (3H, H-26). This genin is known as wistariasapogenol A, already described as the aglycon of saponins of *W. brachybotrys* [13].

Analysis of the HSQC spectrum showed the presence of two anomeric protons at  $\delta_H$  4.45 (d,  $J = 7.6$  Hz) and 4.63 (d,  $J = 7.6$  Hz), giving correlations with two anomeric carbons at  $\delta_C$  103.5 and 103.7 ppm, respectively. According to the same protocol as for compound **1**, a  $\beta$ -D-glucuronopyranosyl and a  $\beta$ -D-xylopyranosyl moieties were identified (Table 1, Figure 1). ROESY correlations have been mainly used to establish the structure of the oligosaccharide chain, between  $\delta_H$  4.45 (1H, GlcA-1)/ $\delta_H$  3.35 (1H, H-3<sub>ax</sub>) and  $\delta_H$  4.63 (1H, Xyl-1)/ $\delta_H$  3.49 (1H, dd,  $J = 9.4, 7.6$  Hz, GlcA-2). Therefore, the structure of compound **2** is established as 3-O- $\beta$ -D-xylopyranosyl-(1 $\rightarrow$ 2)- $\beta$ -D-glucuronopyranosylwistariasapogenol A.

Moreover, five additional known compounds were obtained (**3–7**) (Figure 1), namely 3-O- $\alpha$ -L-rhamnopyranosyl-(1 $\rightarrow$ 2)- $\beta$ -D-xylopyranosyl-(1 $\rightarrow$ 2)- $\beta$ -D-glucuronopyranosylwistariasapogenol A (wistariasaponin A) (**3**) [13], 3-O- $\alpha$ -L-rhamnopyranosyl-(1 $\rightarrow$ 2)- $\beta$ -D-xylopyranosyl-(1 $\rightarrow$ 2)- $\beta$ -D-glucuronopyranosylsoyasapogenol E (wistariasaponin D) (**4**) [11], 3-O- $\alpha$ -L-rhamnopyranosyl-(1 $\rightarrow$ 2)- $\beta$ -D-glucopyranosyl-(1 $\rightarrow$ 2)- $\beta$ -D-glucuronopyranosylsoyasapogenol E (dehydroazukisaponin V) (**5**) [14], 3-O- $\alpha$ -L-rhamnopyranosyl-(1 $\rightarrow$ 2)- $\beta$ -D-xylopyranosyl-(1 $\rightarrow$ 2)- $\beta$ -D-glucuronopyranosylsoyasapogenol B (**6**) (astragaloside VIII) [15], 3-O- $\alpha$ -L-rhamnopyranosyl-(1 $\rightarrow$ 2)- $\beta$ -D-glucopyranosyl-(1 $\rightarrow$ 2)- $\beta$ -D-glucuronopyranosylsoyasapogenol B (azukisaponin V) (**7**) [14].

The sweet taste properties of the saponins with the higher amounts after purification, compounds **1–3**, were evaluated using the stimulation of the human taste heterodimer receptor TAS1R2/TAS1R3, with sucralose as reference ( $EC_{50} = 16 \pm 2$   $\mu$ g/mL). They were applied on a cell-based heterologous expression system and compared to glycyrrhizin. Glycosides **1–3** shared a common oleanane-type aglycone with a primary alcoholic function at the 30-position, a 3-O- $\beta$ -D-glucuronopyranosyl linkage. However, only saponins **2** and **3** activated the sweet taste receptor with  $EC_{50}$  values at  $28 \pm 2$   $\mu$ g/mL and  $29 \pm 7$   $\mu$ g/mL, respectively, both in the same range as glycyrrhizin ( $EC_{50} = 34 \pm 3$   $\mu$ g/mL) (Figure 3). Comparing compound **1** with compounds **2** and **3**, compound **1** possesses a 16 $\beta$ -OH, a

22 $\beta$ -O-acetyl, and a free 24 $\beta$ -CH<sub>3</sub> group, instead of a 22-ketone, a free 16-CH<sub>2</sub>, and a 24 $\beta$ -CH<sub>2</sub>OH function in compounds 2 and 3.

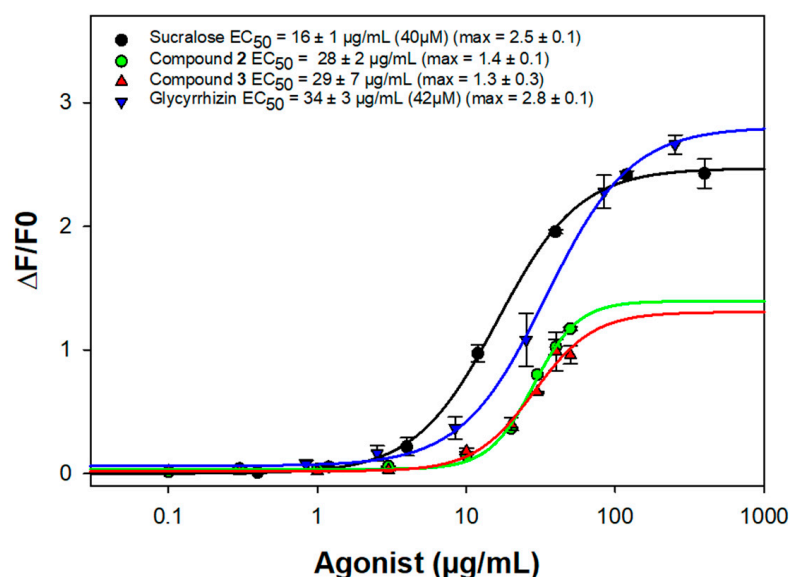


**Figure 3.** Activation of TAS1R2/TAS1R3 by sucralose, compound 2,3 and glycyrrhizin.

Structurally, compounds 2 and 3 shared with glycyrrhizin a 3-O- $\beta$ -D-glucuronopyranosyl linkage, a ketone group, and an oxidated 30 $\beta$ -CH<sub>3</sub> (Figure 1). Previous studies highlighted the key role of the 3-O- $\beta$ -D-glucuronopyranosyl group, the ketone function, and the oxidation of the 24 $\beta$ -CH<sub>3</sub> and the 30 $\beta$ -CH<sub>3</sub> groups [12]. These results are very promising since saponins 2 and 3 can activate the sweet-taste receptor TAS1R2/TAS1R3 with EC<sub>50</sub> values in the micromolar range. These values are close to those measured for sucralose, a sweetener widely used by the food industry, and the glycyrrhizin highly appreciated for its sweetness with a typical licorice taste. However, saponins are known for their toxicity on cell membranes, so, before any further investigations, the toxicity of these molecules has to be evaluated.

### 3. Materials and Methods

#### 3.1. General Experimental Procedures

NMR spectra were recorded on a Varian INOVA 600 MHz spectrometer (Agilent Technologies) equipped with 3 mm triple resonance inverse and 3 mm dual broadband probe heads. Spectra were recorded in methanol-*d*<sub>4</sub>, and all spectra were recorded at T = 308.15 K. Pulse sequences were taken from the Varian pulse sequence library (gCOSY; gHSCAD and gHMBCAD with adiabatic pulses CRISIS-HSQC and CRISIS-HMBC). TOCSY spectra were acquired using DIPSI spin-lock and 150 ms mixing time. Mixing time in ROESY experiments was 300 ms. Chemical shifts were reported in  $\delta$  units and coupling constants (*J*) in Hz. HR-ESIMS (positive-ion mode) and ESIMS (positive- and negative-ion mode) were carried out on a Bruker micrOTOF mass spectrometer. A MARS 6 microwave apparatus (CEM) was used for the extractions. Isolations of the compounds were carried out using column chromatography (CC) with Sephadex LH-20 (550 mm  $\times$  20 mm, GE Healthcare Bio-Sciences AB), and vacuum liquid chromatography (VLC) with reversed-phase RP-18 silica gel (75–200  $\mu$ m, Silicycle). Medium-pressure liquid chromatography (MPLC) was performed using silica gel 60 (Merck, 15–40  $\mu$ m) with a Gilson M 305 pump (25 SC head pump, M 805 manometric module), a Büchi glass column (460 mm  $\times$  25 mm and 460 mm  $\times$  15 mm), and a Büchi precolumn (110 mm  $\times$  15 mm). Thin-layer chromatography (TLC, Silicycle) and high-performance thin-layer chromatography (HPTLC, Merck) were carried out on pre-coated silica gel plates 60 F<sub>254</sub>, solvent system CHCl<sub>3</sub>/MeOH/H<sub>2</sub>O/AcOH (60:32:7:1 and 70:30:5:1). The spray reagent for saponins was vanillin reagent (1% vanillin in EtOH/H<sub>2</sub>SO<sub>4</sub>,



50:1). The HPLC was performed on an Agilent 1260 instrument, equipped with a degasser, a quaternary pump, a sample changer, and a UV detector (210 nm). The chromatographic separation for the analytical part was carried out on a C18 column (250 mm × 4.6 mm internal diameter, 5 µm; Phenomenex LUNA) at room temperature and protected by a guard column. The mobile phase consists of (A) 0.01% (v/v) aqueous trifluoroacetic acid and (B) acetonitrile delivered at 1 mL/min going from 30% to 80% B in 30 min. The injection volume was 10 µL.

### 3.2. Plant Material

*Wisteria sinensis* was purchased from Botanic® (Quetigny, France) in September 2019, and a sample was deposited in the herbarium at the Laboratory of Pharmacognosy, Université de Bourgogne Franche-Comté, Dijon, France, under the number N° 2019/09/06.

### 3.3. Extraction and Isolation

Microwave-assisted extraction of 47.07 g of dried pulverized roots was carried out three times, with a mixture of EtOH/H<sub>2</sub>O (75:35; 500 mL). The microwave apparatus was programmed to reach 60 °C in 10 min, and then maintain this temperature for another 30 min with moderate agitation. After evaporation of the solvent under vacuum, the resulting extract (6.65 g) was submitted to VLC (RP-18 silica gel, H<sub>2</sub>O, MeOH/H<sub>2</sub>O 50:50, and MeOH). The fraction eluted with 50:50 MeOH/H<sub>2</sub>O (1.44 g) was fractionated by CC (Sephadex LH-20, MeOH), to give a fraction rich in saponins (846 mg), which was further fractionated by MPLC on silica gel 60 (15–40 µm, CHCl<sub>3</sub>/MeOH/H<sub>2</sub>O 70:30:5, 60:32:7, 64:40:8, 2.5 mL/min). Fractions F1–F16 were obtained, and F4 (31.4 mg), F8 (93.0 mg), F9 (103.7 mg) and F11 (137.1 mg) were fractionated again by successive MPLC on silica gel RP-18 (MeOH/H<sub>2</sub>O 25:75 to 40:60 and 100:0), to give compounds **1** (5.2 mg), **2** (4.7 mg), wistariasaponin A (**3**) (20.4 mg), wistariasaponin D (**4**) (3.2 mg), dehydroazukisaponin V (**5**) (3.2 mg), astragaloside VIII (**6**) (4.5 mg), and azukisaponin V (**7**) (4.5 mg).

3-*O*-α-*L*-rhamnopyranosyl-(1→2)-β-*D*-glucopyranosyl-(1→2)-β-*D*-glucuronopyranosyl-22-*O*-acetylolean-12-ene-3β,16β,22β,30-tetrol (**1**). White, amorphous powder; <sup>1</sup>H and <sup>13</sup>C NMR data (600 MHz and 150 MHz, MeOD), see Table 1; HR-ESIMS (positive-ion mode) *m/z* 1023.5051 [M + Na]<sup>+</sup> (calcd. for C<sub>50</sub>H<sub>80</sub>O<sub>20</sub>Na, 1023.5141).

3-*O*-β-*D*-xylopyranosyl-(1→2)-β-*D*-glucuronopyranosylwistariasapogenol A (**2**). White, amorphous powder; <sup>1</sup>H and <sup>13</sup>C NMR data (600 MHz and 150 MHz, MeOD), see Table 1; HR-ESIMS (positive-ion mode) *m/z* 803.4195 [M + Na]<sup>+</sup> (calcd. for C<sub>41</sub>H<sub>64</sub>O<sub>14</sub>Na, 803.4194).

### 3.4. Acid Hydrolysis and Absolute Configuration Determination

An aliquot (150 mg) of a rich saponin fraction was hydrolyzed with 2N aqueous CF<sub>3</sub>COOH (25 mL) for 3 h at 95 °C. After extraction with CH<sub>2</sub>Cl<sub>2</sub> (3 × 15 mL), the aqueous layer was evaporated to dryness with H<sub>2</sub>O until neutral to give the sugar residue (55 mg). Glucuronic acid, glucose, xylose and rhamnose were identified by comparison with authentic samples by TLC using CH<sub>3</sub>COOEt/CH<sub>3</sub>COOH/CH<sub>3</sub>OH/H<sub>2</sub>O (65:25:15:15). After purification of these sugars by prep-TLC in the same solvent, the optical rotation of each purified sugar was measured as follows: D-glucuronic acid: *R*<sub>f</sub> = 0.24, [α]<sup>25</sup><sub>D</sub> + 15 (c 0.2, H<sub>2</sub>O), D-glucose: *R*<sub>f</sub> = 0.50, [α]<sup>25</sup><sub>D</sub> + 110 (c 0.2, H<sub>2</sub>O), D-xylose: *R*<sub>f</sub> = 0.60, [α]<sup>25</sup><sub>D</sub> + 85 (c 0.2, H<sub>2</sub>O), and L-rhamnose: *R*<sub>f</sub> = 0.69, [α]<sup>25</sup><sub>D</sub> + 10 (c 0.2, H<sub>2</sub>O).

### 3.5. Bioactivity Assay

We investigated the ability of purified compounds to activate the sweet taste receptor using heterologous expression of TAS1R2/TAS1R3 and functional calcium imaging. As previously described, the cDNAs for TAS1Rs and the plasmid pGP-CMV-GCaMP6S (Addgene #40753) coding for a calcium biosensor, were transiently transfected into HEK293T cells stably expressing the chimeric G-protein subunit Gα16gust44, using Fugene HD (Promega) [6]. Cells transfected only with calcium indicator vector served as negative control. Prior to the stimulation, the transfected cells were washed with C1 buffer (130 mM NaCl, 5 mM

KCl, 10 mM Hepes, 2 mM CaCl<sub>2</sub>, 5 mM sodium pyruvate, pH 7.4). Then, we monitored calcium mobilization following sweet taste receptor activation after automatic injection of test substances with a Molecular Devices FlexStation 3 system. Compounds **2** and **3** were dissolved first at 10 mg/mL in DMSO with good solubility. Further dilutions were prepared in C1 solution. The compounds **2** and **3** were evaluated up to a maximum range of 50 µg/mL, because they elicited non-specific calcium responses in mock-transfected cells at concentration above 100 µg/mL. Data were collected from at least three independent experiments carried out in duplicate. The concentration-response curves were obtained after correction of calcium signals for the response of mock transfected cells and normalization to the fluorescence of cells prior to the stimulation. EC<sub>50</sub> values were calculated using a four-parameter logistic nonlinear regression with equation  $[f(x) = \min + (\max - \min) / (1 + (x/EC_{50})^{nH})]$  with curves fitting of Sigma Plot software.

**Supplementary Materials:** The following supporting information can be downloaded at: <https://www.mdpi.com/article/10.3390/molecules27227866/s1>, The following are available online: Figures S1–S3. <sup>1</sup>H spectrum of compound **1**; Figures S4–S7. <sup>13</sup>C spectrum of compound **1**; Figures S8–S11. HSQC spectrum of compound **1**; Figures S12 and S13. HMBC spectra of compound **1**; Figure S14–S16. COSY spectrum of compound **1**; Figures S17–S19. ROESY spectrum of compound **1**; Figures S20–S22. <sup>1</sup>H spectrum of compound **2**; Figures S23–S26. <sup>13</sup>C spectrum of compound **2**; Figures S27–S30. HSQC spectrum of compound **2**; Figures S31–S34. HMBC spectrum of compound **2**; Figures S35 and S36. COSY spectrum of compound **2**; Figures S37 and S38. ROESY spectrum of compound **2**.

**Author Contributions:** Phytochemical analysis, S.H., A.B., D.P., A.-C.M.-O. and M.-A.L.-D.; NMR and mass spectrometry, T.M. and C.T.; biological assays, C.B. and L.B. All authors have read and agreed to the published version of the manuscript.

**Funding:** This research was supported by a grant from the French Government (French Ministry of Higher Education, Research and Innovation).

**Institutional Review Board Statement:** Not applicable.

**Informed Consent Statement:** Not applicable.

**Data Availability Statement:** Not applicable.

**Conflicts of Interest:** The authors declare no conflict of interest.

**Sample Availability:** Samples of crude extracts are available from the authors.

## References

- Disse, E.; Bussier, A.-L.; Veyrat-Durebex, C.; Deblon, N.; Pfluger, P.T.; Tschöp, M.H.; Laville, M.; Rohner-Jeanrenaud, F. Peripheral ghrelin enhances sweet taste food consumption and preference, regardless of its caloric content. *Physiol. Behav.* **2010**, *101*, 277–281. [CrossRef] [PubMed]
- Fujiwara, S.; Imada, T.; Nakagita, T.; Okada, S.; Nammoku, T.; Abe, K.; Misaka, T. Sweeteners interacting with the transmembrane domain of the human sweet-taste receptor induce sweet-taste synergisms in binary mixtures. *Food Chem.* **2012**, *130*, 561–568. [CrossRef]
- Mennella, J.A.; Bobowski, N.K.; Reed, D.R. The development of sweet taste: From biology to hedonics. *Rev. Endocr. Metab. Disord.* **2016**, *17*, 171–178. [CrossRef] [PubMed]
- Carniel Beltrami, M.; Döring, T.; De Dea Lindner, J. Sweeteners and sweet taste enhancers in the food industry. *Food Sci. Technol.* **2018**, *38*, 181–187. [CrossRef]
- Nakagawa, Y.; Nagasawa, M.; Mogami, H.; Lohse, M.; Ninomiya, Y.; Kojima, I. Multimodal function of the sweet taste receptor expressed in pancreatic β-cells: Generation of diverse patterns of intracellular signals by sweet agonists. *Endocr. J.* **2013**, *60*, 1191–1206. [CrossRef] [PubMed]
- Belloir, C.; Brulé, M.; Tornier, L.; Neiers, F.; Briand, L. Biophysical and functional characterization of the human TAS1R2 sweet taste receptor overexpressed in a HEK293S inducible cell line. *Sci. Rep.* **2021**, *11*, 22238. [CrossRef] [PubMed]
- Azani, N.; Babineau, M.; Bailey, C.D.; Banks, H.; Barbosa, A.R.; Pinto, R.B.; Boatwright, J.S.; Borges, L.M.; Brown, G.K.; Bruneau, A.; et al. A new subfamily classification of the Leguminosae based on a taxonomically comprehensive phylogeny—The Legume Phylogeny Working Group (LPWG). *Taxon* **2017**, *66*, 44–77. [CrossRef]
- Angiosperm Phylogeny Website. Available online: <http://www.mobot.org/MOBOT/Research/APweb/welcome.html> (accessed on 7 June 2022).



9. Champy, A.-S.; Mitaine-Offer, A.-C.; Miyamoto, T.; Tanaka, C.; Papini, A.-M.; Lacaille-Dubois, M.-A. Structural analysis of oleanane-type saponins from the roots of *Wisteria frutescens*: Oleanane-type saponins from *Wisteria frutescens*. *Magn. Reson. Chem.* **2017**, *55*, 595–600. [[CrossRef](#)] [[PubMed](#)]
10. Champy, A.-S.; Mitaine-Offer, A.-C.; Paululat, T.; Papini, A.-M.; Lacaille-Dubois, M.-A. Triterpene saponins from *Wisteria floribunda* “Macrobotrys” and “Rosea”. *Nat. Prod. Commun.* **2017**, *12*, 1573–1576. [[CrossRef](#)]
11. Konoshima, T.; Kozuka, M.; Haruna, M.; Ito, K. Constituents of leguminous plants, XIII. New triterpenoid saponins from *Wistaria brachybotrys*. *J. Nat. Prod.* **1991**, *54*, 830–836. [[CrossRef](#)] [[PubMed](#)]
12. Schmid, C.; Brockhoff, A.; Shoshan-Galeczki, Y.B.; Kranz, M.; Stark, T.D.; Erkaya, R.; Meyerhof, W.; Niv, M.Y.; Dawid, C.; Hofmann, T. Comprehensive structure-activity-relationship studies of sensory active compounds in licorice (*Glycyrrhiza glabra*). *Food Chem.* **2021**, *364*, 130420. [[CrossRef](#)] [[PubMed](#)]
13. Konoshima, T.; Kozuka, M.; Haruna, M.; Ito, K.; Kimura, T.; Tokuda, H. Studies on the constituents of leguminous plants. (XII.1) from *Wistaria brachybotrys* SIEB. et (ZUCC.2) The structures of new triterpenoid saponins. *Chem. Pharm. Bull.* **1989**, *37*, 2731–2735. [[CrossRef](#)]
14. Mohamed, K.M.; Ohtani, K.; Kasai, R.; Yamasaki, K. Oleanene glycosides from seeds of *Trifolium alexandrinum*. *Phytochemistry* **1995**, *40*, 1237–1242. [[CrossRef](#)]
15. Kitagawa, I.; Wang, H.K.; Yoshikawa, M. Saponin and sapogenol. XXXVII.1) Chemical constituents of *Astragali radix*, the root of *Astragalus membranaceus* BUNGE. (4). Astragaloside VII and VIII. *Chem. Pharm. Bull.* **1983**, *31*, 716–722. [[CrossRef](#)]